Inorg. Chem. **2002**, *41*, 3866–3875

Metal–Metal Interactions in Dinuclear d^8 Metal Cyanide Complexes Supported by Phosphine Ligands. Spectroscopic Properties and ab Initio Calculations of $[M_2(\mu\text{-diphosphine})_2(CN)_4]$ and *trans*-$[M(phosphine)_2(CN)_2]$ (M = Pt, Ni)

Bao-Hui Xia, Chi-Ming Che,* David Lee Phillips,† King-Hung Leung, and Kung-Kai Cheung

Department of Chemistry and the HKU-CAS Joint Laboratory on New Materials, The University of Hong Kong, Pokfulam Road, Hong Kong SAR, P.R. China

Received January 25, 2002

Structural, spectroscopic properties on the dinuclear $[M_2(dcpm)_2(CN)_4]$ (M = Pt, **1a**; Ni, **2a,** dcpm = bis(dicyclohexylphosphino)methane) and $[M_2(dmpm)_2(CN)_4]$ (M = Pt, **1b**; Ni, **2b**, dmpm = bis(dimethylphosphino)-methane) and the mononuclear *trans*-$[M(PCy_3)_2(CN)_2]$ (M = Pt, **3**; Ni, **4**, PCy_3 = tricyclohexylphosphine) and theoretical investigations on the corresponding model compounds are described. X-ray structural analyses reveal Pt···Pt and Ni···Ni distances of 3.0565(4)/3.189(1) Å and 2.957(1)/3.209(8) Å for **1a**/**1b** and **2a**/**2b**, respectively. The UV–vis absorption bands at 337 nm (ϵ 2.41 × 10^4 dm^3 mol^{-1} cm^{-1}) for **1a** and 328 nm (ϵ 2.43 × 10^4 dm^3 mol^{-1} cm^{-1}) for **1b** in CH_2Cl_2 are assigned to $^1(5d_\sigma^* \rightarrow 6p_\sigma)$ electronic transitions originating from Pt(II)–Pt(II) interactions. Resonance Raman spectroscopy of **1a**, in which all the Raman intensity appears in the Pt–Pt stretch fundamental (93 cm^{-1}) and overtone bands, verifies this metal–metal interaction. Complexes **1a** and **1b** exhibit photoluminescence in the solid state and solution. For the dinuclear nickel(II) complexes **2a** and **2b**, neither spectroscopic data nor theoretical calculation suggests the presence of Ni(II)–Ni(II) interactions. The intense absorption bands at λ > 320 nm in the UV–vis spectra of **2a** and **2b** are tentatively assigned to d → d transitions.

Introduction

Since the initial report on the fascinating photophysical and photochemical properties of the dinuclear d^8-d^8 complex $[Pt_2(P_2O_5H_2)_4]^{4-}$,[1] there has been continued interest in luminescent dinuclear metal complexes, particularly those with d^8 and d^{10} metal ions.[2] To explain the d^8-d^8 metal interaction, Gray and co-workers first presented a qualitative molecular orbital model (see Figure S1 in the Supporting Information),[3] in which the higher lying nd_{z^2} and $(n+1)p_z$ orbitals combine to yield the nd_σ/d_σ^* and $(n+1)p_\sigma/p_\sigma^*$ MOs (MO = molecular orbital). Many spectroscopic studies on dinuclear Rh(I), Ir(I), and Pt(II) complexes have revealed weak metal−metal bonding interactions in the ground state.[4] This results from mixing of MOs with same symmetry between the nd_σ and $(n+1)p_\sigma$ levels.[5] Extensive spectroscopic and photophysical studies on dinuclear d^8 systems have revealed that there is a net metal−metal single bond in $^{1,3}[(nd_\sigma^*)(n+1)p_\sigma]$ excited states produced upon excitation in the $nd_\sigma^* \rightarrow (n+1)p_\sigma$ transition.[6] Experimental studies[6b,c,e]

* To whom correspondence should be addressed. E-mail: cmche@hku.hk.
† Correspondence on resonance Raman spectroscopy.

(1) Roundhill, D. M.; Gray, H. B.; Che, C.-M. *Acc. Chem. Res.* **1989**, *22*, 55−61.
(2) d^8-d^8: (a) Stiegman, A. E.; Rice, S. F.; Gray, H. B.; Miskowski, V. M. *Inorg. Chem.* **1987**, *26*, 1112−1116. (b) Che, C.-M.; Yam, V. W.-W.; Wong, W.-T.; Lai, T.-F. *Inorg. Chem.* **1989**, *28*, 2908−2910. (c) Yip, H.-K.; Lai, T.-F.; Che, C.-M. *J. Chem. Soc., Dalton Trans.* **1991**, 1639−1641. (d) Bailey, J. A.; Miskowski, V. M.; Gray, H. B. *Inorg. Chem.* **1993**, *32*, 369−370. (e) Yip, H.-K.; Cheng, L.-K.; Cheung, K.-K.; Che, C.-M. *J. Chem. Soc., Dalton Trans.* **1993**, 2933−2938. (f) Navarro, J. A. R.; Romero, M. A.; Salas, J. M.; Quirós, M.; Bahraoui, J. E.; Molina, J. *Inorg. Chem.* **1996**, *35*, 7829−7835. (g) Lai, S.-W.; Chan, M. C.-W.; Cheung, T.-C.; Peng, S.-M.; Che, C.-M. *Inorg. Chem.* **1999**, *38*, 4046−4055. $d^{10}-d^{10}$: (h) King, C.; Wang, J.-C.; Khan, M. N. I.; Fackler, J. P., Jr. *Inorg. Chem.* **1989**, *28*, 2145−2149. (i) Fu, W.-F.; Chan, K.-C.; Miskowski, V. M.; Che, C.-M. *Angew. Chem.* **1999**, *111*, 2953−2955; *Angew. Chem., Int. Ed.* **1999**, *38*, 2783−2785. (j) Che, C.-M.; Mao, Z.; Miskowski, V. M.; Tse, M.-C.; Chan, C.-K.; Cheung, K.-K.; Phillips, D. L.; Leung, K.-H. *Angew. Chem., Int. Ed.* **2000**, *39*, 4084−4088.
(3) Mann, K. R.; Gordon, J. G., II; Gray, H. B. *J. Am. Chem. Soc.* **1975**, *97*, 3553−3555.
(4) (a) Dallinger, R. F.; Miskowski, V. M.; Gray, H. B.; Woodruff, W. H. *J. Am. Chem. Soc.* **1981**, *103*, 1595−1596. (b) Rice, S. F.; Gray, H. B. *J. Am. Chem. Soc.* **1981**, *103*, 1593−1595. (c) Rice, S. F.; Milder, S. J.; Gray, H. B. *Coord. Chem. Rew.* **1982**, *43*, 349−354. (d) Rice, S. F.; Miskowski, V. M.; Gray, H. B. *Inorg. Chem.* **1988**, *27*, 4704−4708.
(5) Smith, D. C.; Gray, H. B. *Coord. Chem. Rev.* **1990**, *100*, 169−181.

10.1021/ic020077j CCC: $22.00
Published on Web 06/26/2002

and theoretical considerations have shown that the simplified MO diagram (see Supporting Information) is inadequate and cannot accurately describe the excited states. A more satisfactory description was given by a valence bond treatment in which the monomer excitations are involved in excitonic dipole−dipole coupling. [6b]

Some theoretical studies on d^8−d^8 metal−metal interactions have previously been undertaken. Alvarez and co-workers[7] performed ab initio calculations on the nature of weak M···M contacts between d^8 square-planar ML_4 molecules and predicted the effect of adding axial groups (along the M−M orientation) on the strength of the M−M interaction. These workers also probed the effect of pyramidality on d^8-ML_4 complexes[8] and proposed a correlation between M···M distances and the degree of pyramidalization at the metal atom.

Metal−metal interactions in oligomeric square-planar Pt(II) complexes have been extensively studied including those of the $[Pt(CN)_4]^{2-}$ chain compounds.[9] The dinuclear complex $[Pt_2(dppm)_2(CN)_4]$ [2b] (**1c**, dppm = bis(diphenylphosphino)methane) was previously synthesized by Che and co-workers to probe the interaction between Pt(phosphine)$_2$(CN)$_2$ moieties. Compared to the numerous spectroscopic works on Pt(II) complexes, less attention has been paid to dinuclear Ni(II) systems and most of the studies have been confined to structural reports. These studies have revealed short intramolecular Ni···Ni distances for some polynuclear Ni(II) complexes. For examples, the Ni···Ni distances in $[Ni_2(form)_4]$ (form = *N*,*N*′-di-*p*-tolylformamidinato),[10a] $[Ni_5(\mu_5\text{-tpda})_4X_2]$ (H_2-tpda = tripyridyldiamine, X = Cl^-, CN^-, N_3^-, or NCS^-),[10b] and $Ni_7(\mu_7\text{-teptra})_4Cl_2$ (H_3-teptra = tetrapyridyltriamine)[10c] are 2.485(2), ca. 2.30−2.40, and 2.215−2.383(2) Å, respectively. These relatively short intermetal distances have stimulated interest regarding the presence of Ni(II)−Ni(II) interaction. Cotton and co-workers had calculated the electronic structure of $Ni_2(HNCHNH)_4$ as a model for $Ni_2(form)_4$.[11] Their treatment indicated that there is no net metal−metal bonding interaction at the "zeroth order" level calculation, despite the rather short Ni···Ni distances. Herein, we describe the structural and spectroscopic properties of dinuclear and mononuclear platinum(II) and nickel(II) cyanide complexes supported by the electron-rich phosphine ligands dmpm (bis(dimethylphosphino)methane), dcpm (bis(dicyclohexylphosphino)methane), and PCy_3 (tricyclohexylphosphine). We have also performed ab initio calculations on the models $[M_2(\mu\text{-}H_2PCH_2PH_2)_2(CN)_4]$ and *trans*-$[M(PMe_3)_2(CN)_2]$ (M = Pt or Ni). We conclude that there is metal−metal interaction in the dinuclear $[Pt_2(\mu\text{-diphosphine})_2(CN)_4]$ complexes. For the $[Ni_2(\mu\text{-phosphine})_2(CN)_4]$ congeners, both experimental data and theoretical calculations provide no evidence for Ni−Ni interaction in the ground state.

Experimental Section

General. The phosphine ligands dcpm, dmpm, and PCy_3 were purchased from Strem. All the chemicals and solvents (AR grade) for synthesis were used as received. The solvents for photophysical studies were purified as previously described.[2g] The resonance Raman apparatus and methods have previously been described.[12] $[Pt_2(dcpm)_2(CN)_4]$ (**1a**) and $[Pt_2(dmpm)_2(CN)_4]$ (**1b**) were synthesized by a modified literature method.[13] The starting materials Pt(L)Cl_2 and Ni(L)Cl_2 (L = dcpm or dmpm) were prepared following procedures similar to that for Pt(dppm)Cl_2[13] and Ni(dppm)Cl_2,[14] respectively. For the preparation of *trans*-$[M(PCy_3)_2(CN)_2]$ (M = Pt, **3**; Ni, **4**), the starting materials $Pt(PCy_3)_2Cl_2$ and $Ni(PCy_3)_2Cl_2$ were prepared by reacting PCy_3 with Pt(COD)Cl_2 and $NiCl_2\cdot 6H_2O$, respectively, and were isolated. ^{1}H and ^{31}P NMR spectra were recorded on a Bruker DPX-500 multinuclear FT-NMR spectrometer. Chemical shifts (δ, ppm) were reported relative to tetramethylsilane (^{1}H NMR) and 85% H_3PO_4 (^{31}P NMR). Infrared spectra were obtained on a Bio-Rad FTS-165 spectrometer. UV−vis spectra were obtained on a Hewlett-Packard 8453 diode array spectrophotometer. Positive ion FAB mass spectra were recorded on a Finnigan MAT95 mass spectrometer.

$[Pt_2(dcpm)_2(CN)_4]$, 1a. A methanolic solution of NaCN (0.03 g, 0.6 mmol) was dropwise added to a methanolic (40 mL) suspension of Pt(dcpm)Cl_2 (0.20 g, 0.3 mmol). After 3 h a colorless solution was obtained. Removal of the solvent gave a white solid. After extraction with CH_2Cl_2, the filtrate was reduced to 5 mL. Diethyl ether was added to give a white precipitate. This was filtered and washed with MeOH and diethyl ether. Crystals suitable for X-ray crystal analysis were obtained by slow diffusion of diethyl ether into dichloromethane solution. Yield: 0.20 g, 85%. ^{1}H NMR (500 MHz, $CDCl_3$): δ 3.03 (t, 4 H; CH_2), 1.25−2.93 (m, 88 H; C_6H_{11}). ^{31}P{^{1}H} NMR (500 MHz, $CDCl_3$): δ 13.75 (t, ^1J(PtP) = 2313.6 Hz). IR (KBr, cm^{-1}): ν 2125 (C≡N). MS (+FAB): *m*/*z* 1310 $[M]^+$, 1284 $[M - CN]^+$. Anal. Calcd for $C_{54}H_{92}N_4P_4Pt_2$: C, 49.44; H, 7.07; N, 4.27. Found: C, 49.01; H, 7.42; N, 4.00.

(6) (a) Che, C.-M.; Butler, L. G.; Gray, H. B.; Crooks, R. M.; Woodruff, W. H. *J. Am. Chem. Soc.* **1983**, *105*, 5492−5494. (b) Smith, D. C.; Miskowski, V. M.; Mason, W. R.; Gray, H. B. *J. Am. Chem. Soc.* **1990**, *112*, 3759−3767. (c) Marshall, J. L.; Hopkins, M. D.; Miskowski, V. M.; Gray, H. B. *Inorg. Chem.* **1992**, *31*, 5034−5040. (d) Miskowski, V. M.; Rice, S. F.; Gray, H. B.; Milder, S. J. *J. Phys. Chem.* **1993**, *97*, 4277−4283. (e) Miskowski, V. M.; Rice, S. F.; Gray, H. B.; Dallinger, R. F.; Milder, S. J.; Hill, M. G.; Exstrom, C. L.; Mann, K. R. *Inorg. Chem.* **1994**, *33*, 2799−2807. (f) Dallinger, R. F.; Carlson, M. J.; Miskowski, V. M.; Gray, H. B. *Inorg. Chem.* **1998**, *37*, 5011−5013. (g) Leung, K. H.; Phillips, D. L.; Che, C.-M.; Miskowski, V. M. *J. Raman Spectrosc.* **1999**, *30*, 987−993.

(7) Novoa, J. J.; Aullón, G.; Alemany, P.; Alvarez, S. *J. Am. Chem. Soc.* **1995**, *117*, 7169−7171.

(8) Aullón, G.; Alemany, P.; Alvarez, S. *Inorg. Chem.* **1996**, *35*, 5061−5067.

(9) (a) Miller, J. S.; Epstein, A. J. *Prog. Inorg. Chem.* **1976**, *20*, 1−151. (b) Miller, J. S. *Extended Linear Chain Compounds*; Plenum: New York, 1982; vols. 1−3. (c) Schindler, J. W.; Fukuda, R. C.; Adamson, A. W. *J. Am. Chem. Soc.* **1982**, *104*, 3596−3600. (d) Gliemann, G.; Yersin, H. *Struct. Bonding* **1985**, *62*, 87−153. (e) Lechner, A.; Gliemann, G. *J. Am. Chem. Soc.* **1989**, *111*, 7469−7475. (f) Miskowski, V. M.; Houlding, V. H. *Inorg. Chem.* **1991**, *30*, 4446−4452. (g) Houlding, V. H.; Miskowski, V. M. *Coord. Chem. Rev.* **1991**, *111*, 145−152. (h) Miskowski, V. M.; Houlding, V. H.; Che, C.-M.; Wang, Y. *Inorg. Chem.* **1993**, *32*, 2518−2524. (i) Bailey, J. A.; Hill, M. G.; Marsh, R. E.; Miskowski, V. M.; Schaefer, W. P.; Gray, H. B. *Inorg. Chem.* **1995**, *34*, 4591−4599.

(10) (a) Cotton, F. A.; Matusz, M.; Poli, R. *Inorg. Chem.* **1987**, *26*, 1472−1474. (b) Wang, C.-C.; Lo, W.-C.; Chou, C.-C.; Lee, G.-H.; Chen, J.-M.; Peng, S.-M. *Inorg. Chem.* **1998**, *37*, 4059−4065. (c) Lai, S.-Y.; Lin, T.-W.; Chen, Y.-H.; Wang, C.-C.; Lee, G.-H.; Yang, M.-H.; Leung, M.-K.; Peng, S.-M. *J. Am. Chem. Soc.* **1999**, *121*, 250−251.

(11) Cotton, F. A.; Matusz, M.; Poli, R.; Feng, X. J. *J. Am. Chem. Soc.* **1988**, *110*, 1144−1154.

(12) Zheng, X.; Phillips, D. L. *J. Chem. Phys.* **1998**, *108*, 5772−5783.

(13) Hassan, F. S. M.; Markham, D. P.; Pringle, P. G.; Shaw, B. L. *J. Chem. Soc., Dalton Trans.* **1985**, 279−283.

(14) Van Hecke, G. R.; Horrocks, W. D., Jr. *Inorg. Chem.* **1966**, *5*, 1968−1974.

Table 1. Crystallographic Data and Structure Refinement for Complexes

	1a·2.5 H_2O	**1b**·H_2O	**2a**·2.5 H_2O	**2b**	**3**	**4**
formula	$C_{54}H_{92}N_4P_4Pt_2$	$C_{14}H_{28}N_4P_4Pt_2$	$C_{54}H_{92}N_4P_4Ni_2$	$C_{14}H_{28}N_4P_4Ni_2$	$C_{38}H_{66}N_2P_2Pt$	$C_{38}H_{66}N_2P_2Ni$
fw	1310.56	766.06	1036.50	493.70	807.99	671.60
cryst syst	monoclinic	triclinic	monoclinic	monoclinic	triclinic	triclinic
space group	*P*2/*a* (No. 13)	$P\bar{1}$ (No. 2)	*P*2/*a* (No. 13)	$P2_1/n$	$P\bar{1}$ (No. 2)	$P\bar{1}$ (No. 2)
a (Å)	18.097(3)	8.757(2)	17.999(3)	9.160(1)	9.927(2)	9.972(2)
b (Å)	14.759(2)	9.149(2)	14.513(3)	11.472(1)	10.274(2)	10.289(2)
c (Å)	23.701(3)	9.149(2)	23.895(1)	10.238(1)	11.050(2)	10.908(2)
α (deg)	90.0	79.58(3)	90.0	90.0	65.23(2)	66.00(2)
β (deg)	99.87(2)	66.63(3)	99.298(7)	90.427(2)	69.80(2)	68.91(2)
γ (deg)	90.0	66.63(3)	90.0	90.0	89.72(2)	89.64(2)
V (Å^3)	6263(1)	617.4(2)	6160(1)	1075.8(2)	947.4(4)	941.0(4)
F(000)	2740	366	2340	512	416	366
μ (cm^{-1})	46.05	115.85	7.55	20.52	38.00	6.28
D_c (g cm^{-3})	1.445	2.110	1.168	1.524	1.416	1.185
$2\theta_{max}$ (deg)	51.1	51.12	50.0	55.06	53.2	53.2
reflns unique	11976	2117	11334	2473	3638	3435
no. of reflns with $I > 3\sigma(I)$	8753	2117[a]	5947	2473[a]	3638	2880
no. of params	597	119	600	160	196	196
R, R_w	0.042, 0.066	0.05, 0.14	0.055, 0.085	0.028, 0.087	0.032, 0.046	0.045, 0.063
GOF	1.76	1.18	2.19	0.73	1.69	1.68
residual *ρ* (e Å^{-3})	+1.18, −1.41	+1.394, −4.456	+0.92, −0.55	+0.461, −0.475	+0.69, −2.02	+0.40, −0.53

[a] Reflections with $I > 2\sigma(I)$.

[Pt_2(dmpm)$_2$(CN)$_4$], 1b. NaCN (0.077 g, 1.6 mmol) in methanol (20 mL) was dropwise added to a suspension of Pt(dmpm)Cl_2 (0.27 g, 0.67 mmol) in methanol (20 mL). After 24 h, removal of solvent from the mixture gave a white solid. The solid was washed with water and diethyl ether and then dried. Extraction with $CHCl_3$ and removal of solvent on a rotary evaporator gave a white powder. Crystals suitable for X-ray structure analysis were obtained by diffusion of diethyl ether into methanol solution. Yield: 0.14 g, 54%. ^{1}H NMR (500 MHz, $CDCl_3$): δ 3.23 (m, 4 H; CH_2); 2.07 (m, 24 H; CH_3). ^{31}P{^{1}H} NMR (500 MHz, $CDCl_3$): δ −18.28 (t, ^1J(PtP) = 2282.90 Hz). IR (KBr, cm^{-1}): ν 2139 (C≡N). MS (+FAB): *m*/*z* 767 [M^+ + 1], 740 [M − CN]$^+$. Anal. Calcd for $C_{14}H_{28}N_4P_4Pt_2$·$CHCl_3$: C, 20.34; N, 6.32; H, 3.30. Found: C, 20.04; N, 6.53; H, 3.34.

[Ni_2(dcpm)$_2$(CN)$_4$], 2a. This compound was prepared and purified in the same manner as that for **1a**. Crystals were obtained by evaporation of a CH_2Cl_2/hexane solution. Yield: 86%. ^{1}H NMR (500 MHz, $CDCl_3$): δ 2.61 (t, 4 H; CH_2), 1.25−2.52 (m, 88 H; C_6H_{11}). ^{31}P{^{1}H} NMR (500 MHz, $CDCl_3$): δ 32.87 (s). IR (KBr, cm^{-1}): ν 2110 (C≡N). MS (+FAB): *m*/*z* 1038 [M^+], 1011 [M − CN + 1]$^+$. Anal. Calcd for $C_{54}H_{92}N_4P_4Ni_2$·H_2O: C, 61.38; N, 5.30; H, 8.97. Found: C, 61.65; N, 4.95; H, 9.40.

[Ni_2(dmpm)$_2$(CN)$_4$], 2b. This complex was prepared and purified similarly to**1b**. Crystals were obtained from slow evaporation of a methanol solution of the complex. Yield: 70%. ^{1}H NMR (500 MHz, $CDCl_3$): δ 2.82 (p, 4 H; CH_2), 1.81 (t, 24 H; CH_3). ^{31}P{^{1}H} NMR (500 MHz, $CDCl_3$): δ 2.89 (s). IR (KBr, cm^{-1}): ν 2119 (C≡N). MS(+FAB): *m*/*z* 493 [M^+], 466 [M − CN + 1]$^+$. Anal. Calcd for $C_{14}H_{28}N_4P_4Ni_2$: C, 34.06; N, 11.35; H, 5.72. Found: C, 33.73; N, 11.36; H, 5.77.

***trans*-[Pt(PCy$_3$)$_2$(CN)$_2$], 3.** Pt(PCy$_3$)$_2$$Cl_2$ (0.130 g, 0.16 mmol) and NaCN (0.018 g, 0.4 mmol) in MeOH (20 mL) were stirred for 4 h to give a white suspension. Removal of solvent produced a white solid. The crude solid was extracted with CH_2Cl_2, and the CH_2Cl_2 extract was concentrated to 5 mL. Addition of diethyl ether gave a white solid, which was washed with MeOH and diethyl ether. Crystals were obtained by slow evaporation of a CH_2Cl_2/hexane solution. Yield: 0.11 g, 87%. ^{1}H NMR (500 MHz, $CDCl_3$): δ 1.19−2.75 (m). ^{31}P{^{1}H} NMR (500 MHz, $CDCl_3$): δ 28.56 (t, ^1J(PtP) = 2193.0 Hz). IR (KBr, cm^{-1}): ν 2124 (C≡N). MS(+FAB): *m*/*z* 807 [M^+ + 1]. Anal. Calcd for $C_{38}H_{66}N_2P_2Pt$·CH_3OH: C, 55.75; N, 3.34; H, 8.40. Found: C, 55.96; N, 2.91; H, 8.27.

***trans*-[Ni(PCy$_3$)$_2$(CN)$_2$], 4.** This complex was prepared and purified by the same method as that for **3**. Crystals were obtained by slow diffusion of diethyl ether into CH_2Cl_2 solution. Yield: 87%. ^{1}H NMR (500 MHz, $CDCl_3$): δ 1.2−2.6 (m). ^{31}P{^{1}H} NMR (500 MHz, $CDCl_3$): δ 38.37 (s). IR (KBr, cm^{-1}): ν 2109 (C≡N). FAB MS: *m*/*z*: 672 [M^+]; 645 [M − CN + 1]$^+$. Anal. Calcd for $C_{38}H_{66}N_2P_2Ni$: C, 67.96; N, 4.17; H, 9.91. Found: C, 68.48; N, 4.19; H, 9.96.

Photophysical Measurements. Steady-state emission and excitation spectra at room temperature and 77 K were measured on a Spex 1681 Flurolog-2 model F111AI fluorescence spectrophotometer equipped with a Hamamatsu R928 PMT detector. The spectra at 77 K in the solid state and in MeOH/EtOH (4:1 v/v) were recorded for samples in quartz tubes immersed in a quartz-walled optical Dewar flask filled with liquid nitrogen. For measurements of solution emission spectra at room temperature, the solutions were subjected to four freeze−pump−thaw cycles prior to the measurements. Emission quantum yields were determined by the method of Demas and Crosby[15] with quinine sulfate in 1.0 N sulfuric acid as the standard (Φ_r = 0.546).

X-ray Crystallography. Crystal data and details of collection and refinement are summarized in Table 1.

Graphite-monochromatized Mo Kα radiation (λ = 0.71073 Å) was used, and all the non-hydrogen atoms were refined anistropically, except for the water molecules of **1a**·2.5H_2O, **1b**·H_2O, and **2a**·2.5H_2O. All the hydrogen atoms were placed at calculation positions without refinement.

For crystals **1a**·2.5H_2O (0.15 × 0.15 × 0.05 mm), **1b**·H_2O (0.30 × 0.2 × 0.1), **2a**·2.5H_2O (0.30 × 0.25 × 0.05 mm), **3** (0.30 × 0.15 × 0.10 mm), and **4** (0.20 × 0.15 × 0.05 mm), the crystal data were collected at 301 K on a MAR diffractometer with a 300 mm image plate detector. The images were interpreted and intensities integrated using the program DENZO.[16] For **1a**, **2a**, **3**, and **4**, their structures were solved by Patterson methods and

(15) Demas, J. N.; Crosby, G. A. *J. Phys. Chem.* **1971**, *75*, 991−1024.
(16) DENZO: In *The HKL Manual—A description of programs DENZO, XDISPLAYF, and SCALEPACK*, written by Gewirth, D., with the cooperation of the program authors Otwinowski, Z., and Minor, W., 1995, Yale University, New Haven, CT.

expanded by Fourier methods (PATTY [17]) and refined by full-matrix least-squares using the software package TeXsan[18] on a Silicon Graphics Indy computer. The crystal data of **2b** (0.20 × 0.12 × 0.10 mm) were collected at 294 K on a Bruker SMART CCD diffractometer. The structures of **1b** and **2b** were determined by direct methods and refined by full-matrix least-squares on F^2 employing the SHELXL97 program[19] on a PC.

Computational Details. Previous theoretical work on a dinuclear gold complex[20] showed that the ab initio MP2 (second-order Møller−Plesset) calculations gave a good representation of the ground-state electronic structure. Here, we also performed ab initio theoretical calculation at the MP2 level on the model molecules. All the calculations were performed using the Gaussian 94 program package[21] on a Silicon Graphics Origin2000 machine. For the sake of simplicity, the ancillary cyclohexyl groups of the phosphine ligands were substituted by hydrogen and methyl for the dinuclear and mononuclear models, respectively. $[Ni_2(\mu\text{-}H_2PCH_2PH_2)_2(CN)_4]$ was set to have a C_i symmetry just like the case of the crystalline form of **2b**; $[Pt_2(\mu\text{-}H_2PCH_2PH_2)_2(CN)_4]$ was set to have a C_2 symmetry (the crystal lattice of **1a** displays pseudo-C_2 symmetry for the repeating unit). The two metal centers were placed on the *Z* axis, and the four phosphorus atoms were put in the *YZ* plane and the four CN groups in the *XZ* plane. The molecule *trans*-$[M(PMe_3)_2(CN)_2]$ (M = Pt or Ni) was put in the *XY* plane with the phosphorus atoms on the *X* axis and CN on the *Y* axis; the molecule is of C_{2h} symmetry. We employed the quasi-relativistic pseudopotentials for Pt, Ni, and P by Hay and Wadt,[22] with 19, 19, and 5 valence electrons, respectively; the double-ζ LANL2DZ basis sets associated with the pseudopotentials were adopted. For $[M_2(\mu\text{-}H_2PCH_2PH_2)_2(CN)_4]$ (M = Pt or Ni), the LANL2DZ basis sets were adopted for C, N, and H atoms; while for the monomer systems the standard 6−31g* basis sets were adopted for C, N, and H atoms, and a d-polarization function was added to the P atoms (α_d = 0.334[23]). The basis sets were taken as Pt(8s6p3d)/[3s3p2d], Ni-(8s6p3d)/[3s3p2d], P(3s3p)/[2s2p], C(10s5p)/[3s2p], N(10s5p)/[3s2p], and H(4s)/[2s] for $[M_2(\mu\text{-}H_2PCH_2PH_2)_2(CN)_4]$ (M = Pt or Ni); for *trans*-$[M(PMe_3)_2(CN)_2]$ (M = Pt or Ni), we adopted P(3s3p1d)/[2s2p1d], C(10s4p1d)/[3s2p1d], N(10s4p1d)/[3s2p1d], and H(4s)/[2s]. Thus, the calculations employed 190 basis functions and 132 electrons for $[M_2(\mu\text{-}H_2PCH_2PH_2)_2(CN)_4]$ (M = Pt, Ni) and 224 basis functions and 108 electrons for *trans*-$[M(PMe_3)_2(CN)_2]$ (M = Pt, Ni). The molecular structures were partially optimized.

Table 2. Selected Bond Distances (Å) and Angles (deg)

	1a·2.5H_2O		
Pt(1)−P(1)	2.340(2)	Pt(1)−C(1)	2.003(8)
Pt(2)−P(3)	2.329(2)	Pt(2)−C(4)	1.985(9)
N(1)−C(1)	1.16(1)	N(3)−C(3)	1.10(1)
Pt(1)···Pt(2)	3.0565(4)		
Pt(1)···Pt(2)−P(3)	88.84(5)	Pt(2)···Pt(1)−C(1)	87.6(2)
Pt(2)···Pt(1)−P(1)	91.57(5)	Pt(1)···Pt(2)−C(3)	96.5(3)
P(1)−Pt(1)−P(2)	177.25(7)	P(3)−Pt(2)−P(4)	177.34(8)
P(1)−Pt(1)−C(1)	88.8(2)	P(3)−Pt(2)−C(4)	94.7(3)
C(1)−Pt(1)−C(2)	177.4(3)	C(3)−Pt(2)−C(4)	175.8(4)
	1b·H_2O[a,b]		
Pt(1)−P(1)	2.313(5)	Pt(1)−P(2)	2.310(5)
Pt(1)−C(1)	2.02(3)	Pt(1)−C(2)	1.98(2)
N(1)−C(1)	1.17(4)	N(2)−C(2)	1.20(4)
Pt(1)···Pt(1)*	3.189(1)		
Pt(1)*···Pt(1)−P(1)	89.8(1)	Pt(1)*···Pt(1)−P(2)	88.7(1)
C(1)−Pt(1)−P(1)	87.8(8)	C(2)−Pt(1)−P(2)	87.5(7)
N(1)−C(1)−Pt(1)	169(3)	N(2)−C(2)−Pt(1)	178(3)
C(2)−Pt(1)−C(1)	175.6(7)	P(1)−Pt(1)−P(2)	178.3(1)
	2a·2.5H_2O		
Ni(1)−P(1)	2.241(2)	Ni(2)−P(3)	2.231(2)
Ni(1)−C(1)	1.867(8)	Ni(2)−C(3)	1.860(9)
N(1)−C(1)	1.147(9)	N(3)−C(3)	1.151(9)
Ni(1)···Ni(2)	2.957(1)		
Ni(2)···Ni(1)−P(1)	92.39(5)	Ni(2)···Ni(1)−C(1)	97.2(2)
Ni(1)···Ni(2)−P(3)	89.50(5)	Ni(1)···Ni(2)−C(3)	86.8(2)
P(1)−Ni(1)−P(2)	174.39(7)	P(3)−Ni(2)−P(4)	178.58(8)
P(1)−Ni(1)−C(1)	89.9(2)	P(3)−Ni(2)−C(3)	85.5(2)
C(1)−Ni(1)−C(2)	177.8(3)	C(3)−Ni(2)−C(4)	173.9(3)
	2b[b]		
Ni(1)−P(1)	2.1945(4)	Ni(1)−P(2)	2.2023(4)
Ni(1)−C(1)	1.870(1)	Ni(1)−C(2)	1.860(1)
P(1)−C(3)	1.828(1)	P(2)−C(3A)	1.836(1)
N(1)−C(1)	1.143(2)	N(2)−C(2)	1.146(2)
Ni(1)···Ni(2)	3.209(8)		
Ni(1A)···Ni(1)−P(1)	86.1	Ni(1A)···Ni(1)−P(2)	92.3
C(1)−Ni(1)−P(1)	90.50(4)	C(2)−Ni(1)−P(1)	89.05(4)
C(1)−Ni(1)−P(2)	91.29(4)	C(2)−Ni(1)−P(2)	89.29(4)
N(1)−C(1)−Ni(1)	178.40(1)	N(2)−C(2)−Ni(1)	173.4(1)
C(2)−Ni(1)−C(1)	170.47(6)	P(1)−Ni(1)−P(2)	178.09(1)

[a] This molecule is disordered against the Pt−Pt orientation, i.e., rotated along the bond ca. 51°, only one set of possible structural data is described here. [b] This molecule has an inversion center.

Results and Discussion

Syntheses. The diphosphine ligands dcpm and dmpm have been selected for the syntheses of dinuclear Ni(II) and Pt(II) complexes. Unlike the widely used dppm ligand, the dcpm and dmpm ligands are optically transparent in the UV region. Therefore, it is feasible to probe for metal−metal bonded electronic transitions at shorter wavelengths than for dppm complexes. We prepared $[Pt_2(dcpm)_2(CN)_4]$ (**1a**) and $[Pt_2(dmpm)_2(CN)_4]$ (**1b**) by slight modification of Shaw's method.[13] $[Ni_2(dcpm)_2(CN)_4]$ (**2a**) and $[Ni_2(dmpm)_2(CN)_4]$ (**2b**) were similarly synthesized, which are rare examples of face-to-face dinuclear Ni(II) complexes with bridging diphosphine ligands. To aid spectral assignment, we have also prepared and studied the spectroscopic properties of the monomeric congeners *trans*-$[M(PCy_3)_2(CN)_2]$ (M = Pt, **3**; Ni, **4**).

X-ray Crystal Structures. Selected bond distances and angles of dinuclear compounds are listed in Table 2. Because

(17) PATTY: Beurskens, P. T.; Admiraal, G.; Beurskens, G.; Bosman, W. P.; Garcia-Granda, S.; Gould, R. O.; Smits, J. M. M.; Smykalla, C. The *DIRDIF Program System, Technical Report of the Crystallography Laboratory*; University of Nijmegen: Nijmegen, The Netherlands, 1992.

(18) *TeXsan*: *Crystal Structure Analysis Package*; Molecular Structure Corporation: The Woodlands, TX, 1985 and 1992.

(19) SHELX97: Sheldrick, G. M. *Programs for Crystal Structure Analysis*, Release 97-2; University of Göttingen: Göttingen, Germany, 1997.

(20) Zhang, H.-X.; Che, C.-M. *Chem. Eur. J.* **2001**, *7*, 4887−4893.

(21) Frisch, M. J.; Trucks, G. W.; Schlegel, H. B.; Gill, P. M. W.; Johnson, B. G.; Robb, M. A.; Cheeseman, J. R.; Keith, T.; Petersson, G. A.; Montgomery, J. A.; Raghavachari, K.; Al-Laham, M. A.; Zakrzewski, V. G.; Ortiz, J. V.; Foresman, J. B.; Cioslowski, J.; Stefanov, B. B.; Nanayakkara, A.; Challacombe, M.; Peng, C. Y.; Ayala, P. Y.; Chen, W.; Wong, M. W.; Andres, J. L.; Replogle, E. S.; Gomperts, R.; Martin, R. L.; Fox, D. J.; Binkley, J. S.; Defrees, D. J.; Baker, J.; Stewart, J. P.; Head-Gordon, M.; Gonzalez, C.; Pople, J. A. *Gaussian 94*, Revision C.3; Gaussian, Inc.: Pittsburgh, PA, 1995.

(22) (a) Wadt, W. R.; Hay, P. J. *J. Chem. Phys.* **1985**, *82*, 284−298. (b) Hay, P. J.; Wadt, W. R. *J. Chem. Phys.* **1985**, *82*, 299−310.

(23) Check, C. E.; Faust, T. O.; Bailey, J. M.; Wright, B. J.; Gilbert, T. M.; Sunderlin, L. S. *J. Phys. Chem. A* **2001**, *105*, 8111−8116.

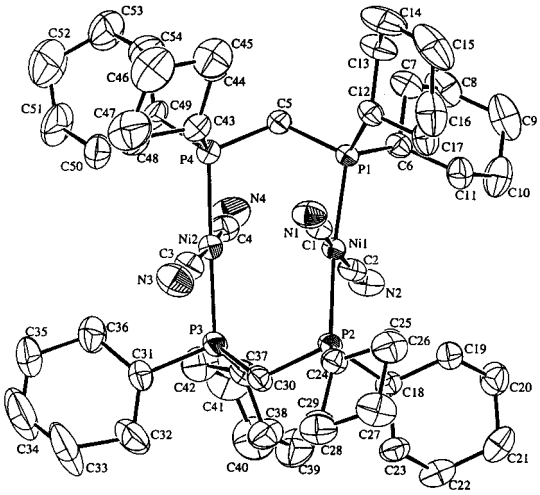

Figure 1. ORTEP drawing of complex **2a** with thermal ellipsoids on the 40% probability level (hydrogen atoms are not shown) and the numbering scheme.

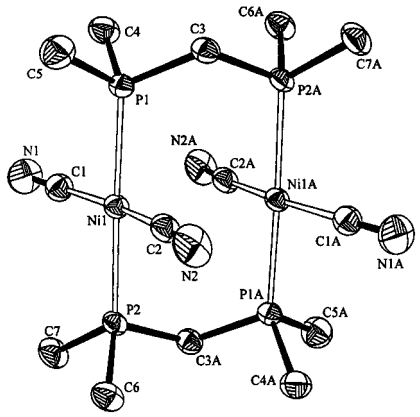

Figure 2. ORTEP drawing of complex **2b** with thermal ellipsoids on the 50% probability level (hydrogen atoms are not shown) and the numbering scheme.

1a/**2a**, **1b**/**2b** are isostructural, only the ORTEP drawings of **2a** and **2b** are shown (see Figures 1 and 2, respectively). The other crystal structural data and ORTEP drawings are given in the Supporting Information.

The structures of **3** and **4** are similar. Each metal atom exhibits square-planar *trans*-$[MP_2(CN)_2]$ (P, phosphine ligand) coordination. The M−P and M−C distances in **3**/**4** are 2.336(1)/2.2426(6) Å and 2.021(5)/1.857(3) Å, respectively.

Complexes **1a**, **1b**, **2a**, and **2b** are structurally related to $[Pt_2(dppm)_2(CN)_4]$ (**1c**)[2b] and $[Pd_2(dppm)_2(CN)_4]$,[2c] while **1b** and **2b** contain a crystallographically imposed center of symmetry. In these four complexes, each metal atom exhibits square-planar geometry with two *trans*-cyano groups and two *trans*-P atoms from bridging diphosphine ligands. The two $MP_2(CN)_2$ units in all of the dimers are in normal face-to-face orientation. However, the two $MP_2(CN)_2$ units in **1a** and **2a** are not eclipsed but skewed to each other with dihedral angles P−M−M−P/C−M−M−C of ca. 23.1/28.1 (**1a**) and 21.99°/27.6° (**2a**), respectively, which are different from that in **1b**, **2b**, and other $[M_2(dppm)_2(CN)_4]$ (M = Pt or Pd) analogues. Such a structural difference between the dmpm-, dppm-, and dcpm-bridged metal complexes is attributed to the steric bulkiness of the dcpm ligand which disfavors face-to-face arrangement of neighboring $MP_2(CN)_2$ moieties. All the P−M−P angles fall between 174.39(7)° and 178.58(8)°. The C−M−C angles of 173.9(3)−177.8(3)° in **1a**, **1b**, and **2a** are larger than that in **2b** (170.47(6)°). Indeed, the $NiP_2(CN)_2$ units in **2b** are significantly distorted from square-planar geometry. The average Pt−C distances of 2.008/2.00 Å and Pt−P distances of 2.334/2.312 Å in **1a**/**1b** respectively are comparable to those values found in **1c** (Pt−C = 2.003 Å, Pt−P = 2.322 Å) and **3** (see above). In **2a** and **2b**, the average Ni−C distances (1.873 and 1.865 Å, respectively) and the average Ni−P distances (2.236 and 2.1984 Å, respectively) are comparable to the average Ni−C distances of 1.868 Å[24a] in $[CdNi(CN)_4(C_6H_8N_2)(NH_3)]$ and Ni−P distances of 2.185 Å[24b] in *cis*-[Ni(tdppcyme)Cl_2] (tdppcyme = *cis*,*cis*-1,3,5-$(PPh_2)_3$-1,3,5-$(COOCH_3)_3$-C_6H_5).

The intriguing structural feature is the intramolecular M···M distance in each structure. The Pt···Pt distance in **1a** and **1b** is 3.0565(4) and 3.189(1) Å, respectively, which are relatively shorter than the value of 3.301(1) Å in **1c**[2b] but slightly longer than that of 2.925(1) Å in $[Pt_2(P_2O_5H_2)_4]^{4-}$.[25] Miller[9a] noted that for monomeric square-planar Pt(II) complexes stacked to form a continuous chain of metal atoms, the Pt···Pt distances lie in the range 3.09−3.50 Å. Hence, the Pt···Pt distances in **1a** and **1b** suggest the presence of weak Pt−Pt interactions.

The Ni···Ni distances in **2a** and **2b** are 2.957(1) and 3.209(8) Å, respectively. They are comparable to the Ni···Ni separations of 3.207(6) Å in $[Ni(dmgBF_2)]_2$[26a] ($dmgBF_2$ = difluoroborondimethylglyoximato) and 3.298 Å[26b] in $[Ni_2L_3]^{2-}$ (L = biphenyl-2,2′-dithiolate). However, they are significantly longer than the Ni···Ni distances in some polynuclear Ni(II) complexes, including those mentioned in the Introduction as well as in the linear chain $[Ni_3(bipyam\text{-}H)_4Cl_2]$ unit[27a] (2.443(1) and 2.431(1) Å, bipyam-H = bis(2-pyridyl)-amide) and in $[Ni_5(\mu_5\text{-}tpda)_4Cl_2]$[27b] (2.385(2) and 2.305(1) Å, H_2-tpda = tripyridyldiamine).

It is noteworthy that, irrespective of the metal atom, the M···M distances of the dmpm-bridged complexes are longer than those of the dcpm-bridged analogues, i.e., **1b** > **1a** and **2b** > **2a**. According to previous work,[28] the cone angles of the diphosphine ligands are in the order dcpm > dppm > dmpm. The dcpm ligand is more bulky than dmpm, which results in twisting of the two $MP_2(CN)_2$ units away from an eclipsed configuration, and hence closer proximity for the two metal atoms. The Pt···Pt distance for **1c** (with dppm ligand) is the longest among the three complexes **1a**, **1b**,

(24) (a) Hökelek, T.; Ülkü, D. *Acta Crystallogr., Sect. C* **1988**, *44*, 832−834. (b) Heins, M.; Stössel, P.; Mayer, H. A.; Fawzi, R.; Steimann, M. *J. Organomet. Chem.* **1999**, *587*, 258−266.
(25) Dos Remedios Pinto, M. A. F.; Sadler, P. J.; Neidle, S.; Sanderson, M. R.; Subbiah, A.; Kuroda, R. *J. Chem. Soc., Chem. Commun*. **1980**, 13−15.
(26) (a) Stephens, F. S.; Vagg, R. S. *Acta Crystallogr., Sect. B* **1977**, *33*, 3159−3164. (b) Erkizia, E.; Conry, R. R. *Inorg. Chem.* **2000**, *39*, 1674−1679.
(27) (a) Aduldecha, S.; Hathaway, B. *J. Chem. Soc., Dalton Trans.* **1991**, 993−998. (b) Shieh, S.-J.; Chou, C.-C.; Lee, G.-H.; Wang, C.-C.; Peng, S.-M. *Angew. Chem.* **1997**, *109*, 57−59; *Angew. Chem., Int. Ed. Engl.* **1997**, *36*, 56−59.
(28) Tolman, C. A. *Chem. Rev.* **1977**, *77*, 313−348.

Table 3. Spectroscopic and Photophysical Properties of **1a**−**4**

complex	medium (*T*/K)	λ_{abs}/nm (ϵ /dm^3 mol^{-1} cm^{-1})	λ_{em}/nm (τ/μs)[a]
$[Pt_2(dcpm)_2(CN)_4]$, **1a**	CH_2Cl_2[b]	263 (8900), 337 (24100), 388 (300)	386,[c] 448 (0.1)
	glass (77)[d]		380,[c] 448 (2.6)
	solid (298)		388,[c] 450 (0.2)
	solid (77)		388,[c] 450 (3.0)
$[Pt_2(dmpm)_2(CN)_4]$, **1b**	CH_2Cl_2	235 (6000), 256 (6000), 328 (24300), 375 (50)	nonemissive
	glass (77)[d]		438 (3.6)
	solid (298)		444 (1.0)
	solid (77)		442 (2.9)
$[Ni_2(dcpm)_2(CN)_4]$, **2a**	CH_2Cl_2	251 (55400), 306 (5300), 361 (3700), 391 (3900)	nonemissive
	MeOH	252 (53000), 306 (6400), 358 (3900), 395 (4900)	nonemissive
$[Ni_2(dmpm)_2(CN)_4]$, **2b**	MeOH	240 (66200), 267 (6600), 298 (5300), 342 (4700), 380 (3600)	nonemissive
$[Pt(PCy_3)_2(CN)_2]$, **3**	CH_2Cl_2	231 (6300), 251 (6600), 260 (6200), 273 (2900), 289 (1400)	nonemissive
$[Ni(PCy_3)_2(CN)_2]$, **4**	CH_2Cl_2	264 (49600), 294 (8500), 312 (2900), 344 (700)	nonemissive

[a] For emission spectra measurements excitation wavelength: 338 nm for **1a**, 330 nm for **1b**. For luminescence lifetime measurements: excitation at 355 nm. [b] The emission quantum yield is 1.68×10^{-3}. [c] The lifetime for the higher-energy emissions cannot be measured due to the limitation ($\tau < 10$ ns) of the instrument. [d] Solvent: EtOH/MeOH (1:4 v/v).

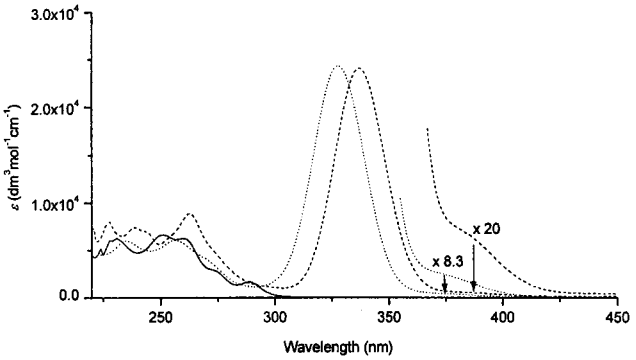

Figure 3. UV−vis absorption spectra of **1a** (- - -), **1b** (···), and **3** (—) in CH_2Cl_2 at room temperature.

and **1c**. It thus appears that both electronic and steric effects of the bridging diphosphine auxiliaries affect the M···M distances.

Absorption Spectra and Photophysical Properties. (a) Platinum(II) Complexes. Spectroscopic and photophysical data are set out in Table 3. The electronic absorption spectra of **1a**, **1b**, and **3** are shown in Figure 3. In dichloromethane, the monomeric *trans*-$[Pt(PCy_3)_2(CN)_2]$ **3** shows absorption bands at 231 (ϵ 6300 dm^3 mol^{-1} cm^{-1}), 251 (6600), 260 (6200), 273 (2900), and 289 nm (1400), which are very similar to the spectral data reported for *trans*-$[Pt(P(n\text{-}Bu_3)_2(CN)_2]$ by Mason et al.[29] These bands are clearly electrically dipole-allowed because their extinction coefficients are greater than 10^3 dm^3 mol^{-1} cm^{-1} (thus excluding assignments to d−d transitions, which are Laporte forbidden). The spectroscopic assignments for complexes of this type, as well as of their homoleptic congeners $[Pt(CN)_4]^{2-}$ and $[Pt(phosphine)_4]^{2+}$, have been extensively discussed in the literature.[29,30] There is general agreement that the transitions relate to states of the type $^{1,3}\{[5d(Pt)][6p_z(Pt),\pi^*(L)]\}$ (L = CN^-, PR_3), but the relative importance of the ligand contributions to the terminal orbital is not well established in most cases. As emphasized by Mason,[29,30c] the group-theoretical classification of the excited states is largely independent of the various assumptions about the nature of the terminal orbital. The close similarity for the spectra of $[Pt(CN)_n(PR_3)_{4-n}]^{2-n}$ ($n = 0, 2$), all of which show a series of UV bands between 300 and 220 nm with ϵ 1−6 $\times$ 10^3 dm^3 mol^{-1} cm^{-1}, suggests a dominant $6p_z$(Pt) contribution. This is similar to the well-established dominant $(n + 1)p_z$(M) contribution in analogous transitions of valence-isoelectronic Rh(I) and Ir(I) complexes.[6b] However, the very complicated spectrum of the low-symmetry compound **3** does not contribute to our understanding. We note that older literature[29] assumes that the $\pi^*(PR_3)$ levels derive from 3d(P) orbitals. Theoretical discussions[31] including calculations performed by us (vide infra) indicate that 3d(P) orbitals play no significant role in bonding or in the composition of the low-energy states. However, the σ^*(P−R) orbitals lie at relatively low energy and can play a role as π^*-acceptor orbitals.[31d]

The electronic spectra of dinuclear **1a** and **1b** are similar to that of **3** for $\lambda < 300$ nm, but differ dramatically by exhibiting an intense band at 337 nm (ϵ 24100 dm^3 mol^{-1} cm^{-1}) for **1a** and 328 nm (ϵ 24300) for **1b**. The bands also show a weak, long-wavelength shoulder (**1a** 388 nm (ϵ 300 dm^3 mol^{-1} cm^{-1}); **1b** 375 nm (ϵ 50)) that can be assigned to spin-forbidden analogues of the intense band. These absorption bands are comparable to the spin-allowed and spin-forbidden $d_\sigma^* \rightarrow p_\sigma$ transitions of the $[Pt_2(dppm)_2(CN)_4]$ analogue, which occurs at 324 and 390 nm, respectively.[2b] The inferred singlet−triplet excited-state splittings for **1a** and **1b** are ∼4000 cm^{-1}, which are comparable to the corresponding value of 4259 cm^{-1} in $[Pt_2(P_2O_5H_2)_4]^{4-}$.[1]

The compounds also exhibit intense luminescence (Figure 4). Complex **1b** only emits in rigid media (glassy solutions or crystalline solid) with lifetimes of ∼1.0−4.0 μs for the single ∼440 nm emission, indicating phosphorescence from the triplet excited state. Complex **1a** differs by emitting weakly in fluid solution, and also exhibiting two emissions. The 450 nm emission with lifetime in the microsecond region

(29) Solar, J. M.; Ozkan, M. A.; Isci, H.; Mason, W. R. *Inorg. Chem.* **1984**, *23*, 758−764.

(30) (a) Mason, W. R., III; Gray, H. B. *J. Am. Chem. Soc.* **1968**, *90*, 5721−5729. (b) Piepho, S. B.; Schatz, P. N.; McCaffery, A. J. *J. Am. Chem. Soc.* **1969**, *91*, 5994−6001. (c) Isci, H.; Mason, W. R. *Inorg. Chem.* **1975**, *14*, 905−912. (d) Cowman, C. D.; Gray, H. B. *Inorg. Chem.* **1976**, *15*, 2823−2824.

(31) (a) Xiao, S.-X.; Trogler, W. C.; Ellis, D. E.; Berkovitch-Yellin, Z. *J. Am. Chem. Soc.* **1983**, *105*, 7033−7037. (b) Marynick, D. S. *J. Am. Chem. Soc.* **1984**, *106*, 4064−4065. (c) Pacchioni, G.; Bagus, P. S. *Inorg. Chem.* **1992**, *31*, 4391−4398. (d) Gilheany, D. G. *Chem. Rev.* **1994**, *94*, 1339−1374.

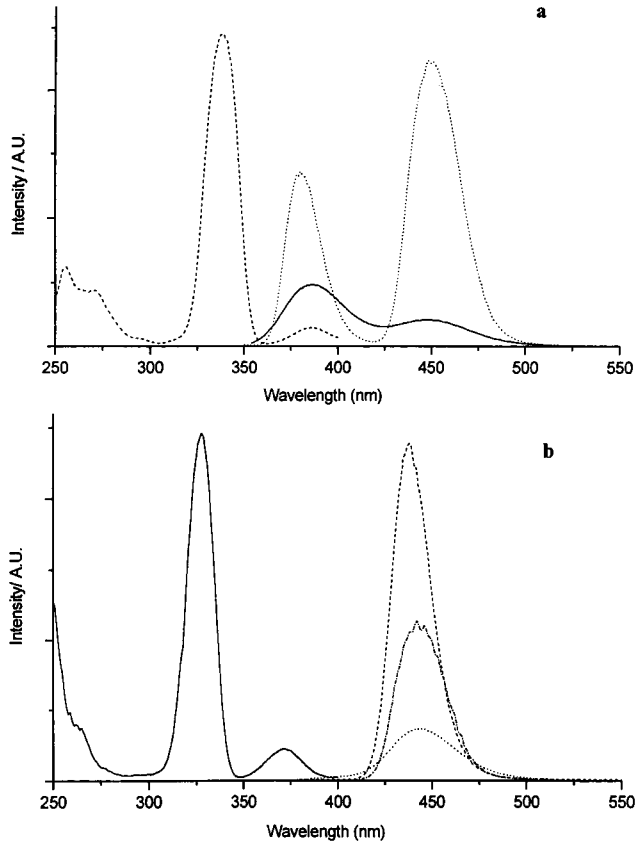

Figure 4. (a) The excitation (- - -) and emission spectra (·····) in the glass state (MeOH/EtOH 4:1 v/v) at 77 K and the emission spectrum in CH_2Cl_2 (—) at room temperature of **1a**. (b) The excitation (—) and emission (- - -) spectra in the glass state (MeOH/EtOH 4:1 v/v) at 77 K and emission spectrum in the solid state at 77 K (-·-·) and room temperature (···) of **1b**.

is attributable to phosphorescence, while the shorter wavelength band at ~386 nm with lifetime <10 ns is assigned to fluorescence from the singlet excited state.

These photophysical properties are diagnostic for dinuclear d^8-d^8 $^{1,3}[d_\sigma^* \rightarrow p_\sigma]$ excited states.[1,3,4,6] The $^{1,3}[nd_{z^2}(M) \rightarrow (n+1)p_z(M)]$ transitions are specifically perturbed by ground- and excited-state interactions; as a result, the $^{1,3}[nd_\sigma^* \rightarrow (n+1)p_\sigma]$ components of $^{1,3}[nd_{z^2}(M) \rightarrow (n+1)p_z(M)]$ are strongly stabilized,[6] whereas effects upon other $nd(M) \rightarrow ((n+1)p(M), \pi^*(L))$ transitions are minor.[6b]

Unlike for dinuclear Rh(I) and Ir(I) isocyanide complexes,[6] there is no clear correlation of the dinuclear Pt(II) ~330 nm band to a $^1[nd_{z^2} \rightarrow (n+1)p_z]$ transition for monomer **3**. Indeed, it is possible that $nd_{z^2} \rightarrow (n+1)p_z$ character may be spread over several transitions for **3**, owing to mixing of p_z(Pt) with π^*(L) orbitals. The resonance Raman results presented below suggest pure $^1[nd_\sigma^* \rightarrow (n+1)p_\sigma]$ character for the ~330 nm band of the dinuclear complexes, perhaps because energetic resolution of the low-energy transitions results in reduced metal−ligand mixing.

The energetic ordering of the low-energy Pt(II)−Pt(II) bands tracks the Pt···Pt distance; a shorter distance by 0.1325 Å (Table 2) results in a $^1[nd_\sigma^* \rightarrow (n+1)p_\sigma]$ transition energy that is blue-shifted by ~800 cm^{-1}, consistent with a weaker Pt−Pt interaction. Correlations of this type have been clearly demonstrated for the absorption/emission spectra of linear-chain $[Pt(CN)]_4^{2-}$ compounds[9d] and other dinuclear Pt(II) complexes.[2d]

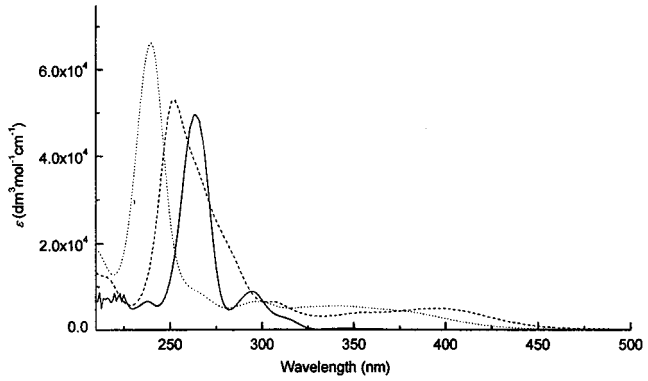

Figure 5. UV−vis absorption spectra of **2a** (- - -) and **2b** (···) in CH_3OH and **4** (—) in CH_2Cl_2 at room temperature.

(b) Ni(II) Complexes. The electronic absorption spectra of **2a**, **2b**, and **4** are shown in Figure 5. No luminescence was detected from these compounds.

The spectrum of **4** is very similar to that reported for *trans*-$[Ni(PEt_3)_2(CN)_2]$.[29] Like **3** and related Pt(II) complexes, **4** displays a complicated spectrum consisting of a series of absorption bands with ϵ values around 10^3 dm^3 mol^{-1} cm^{-1} at $\lambda \leq 320$ nm. There is a clear difference, however, in that **4** also displays a very intense (ϵ 49600 dm^3 mol^{-1} cm^{-1}) band at 264 nm. For the dinuclear **2a** and **2b** derivatives, this band is blue-shifted by 1900 and 3800 cm^{-1}, respectively. There is certainly no correlation with Ni···Ni distances. However, there is a correlation with Ni−P distances, whose average values are 2.243 Å (**4**) > 2.236 Å (**2a**) > 2.198 Å (**2b**). Thus, the transition energy decreases as the Ni−P distance increases.

Comparisons to the spectra of homoleptic complexes are informative. The spectrum of the complex $[Ni(CN)_4]^{2-}$ does not exhibit an analogous band; it is, in fact, very similar to the spectrum of $[Pt(CN)_4]^{2-}$. The spectra of Ni(II) phosphine complexes do display comparable bands; for example, $[Ni(bis(diethylphosphino)ethane)_2]^{2+}$ has a band at 252 nm (ϵ 34500 dm^3 mol^{-1} cm^{-1}).[29] Clearly, this band is associated with the Ni−P unit.

The absence of a similar transition for Pt(II) complexes suggests that it is strongly blue-shifted for the third transition series. Such behavior is incompatible for d(M) → p(M) or MLCT (metal-to-ligand charge-transfer) transitions, but is consistent with an LMCT (ligand-to-metal charge-transfer) assignment.[30a] The obvious assignment is $P(\sigma) \rightarrow Ni(d_{x^2-y^2})$. Such an LMCT assignment does not appear to have been previously considered for this band, but is reasonable for the first transition series metal ion considering the strongly reducing nature of phosphines. In any case, the UV bands are clearly unrelated to the nature of the Ni−Ni interactions.

The spectra of dinuclear **2a** and **2b** show a number of moderately intense bands ($\epsilon \sim 4000$ dm^3 mol^{-1} cm^{-1}) in the 300−450 nm region that are not evident in the monomer spectrum. However, assignment of these bands to Ni−Ni transitions is confounded both by their weakness and by their number (there is only one $^1(d_\sigma^* \rightarrow p_\sigma)$ transition).

In fact, low-spin square-planar Ni(II) complexes do display very weak transitions ($\epsilon \sim 10^{1-3}$ dm^3 mol^{-1} cm^{-1}) in the visible region with d−d transitions terminating in the empty $d_{x^2-y^2}$ orbital. Such transitions are strongly blue-shifted for Pt(II).[30a]

The most thoroughly examined case is the $[Ni(CN)_4]^{2-}$ complex, which has been examined by solution absorption and MCD spectroscopy[30a,b] and single-crystal absorption spectroscopy.[30d,32] Bands have been located at 310 (ϵ 700 dm^3 mol^{-1} cm^{-1}), 330 (ϵ 500), 370, 440 ($\epsilon \sim 2$), and 500 nm. The third and fifth of these were only evident in the single-crystal spectra.[32] Detailed assignments are not available for these bands, and singlet−triplet assignments may be applied for some,[30a] particularly the very weak 440 and 500 nm bands.

Nevertheless, the important point is that d−d transitions are known to occur in the visible to near UV region for $[Ni(CN)_4]^{2-}$. Since phosphines are weaker-field ligands than cyanide, d−d transitions should actually be red-shifted for *trans*-$[Ni(PR_3)_2(CN)_2]$ complexes. We therefore assign the 300−450 nm bands of **2a** and **2b** to d−d transitions.

The reason for the weakness of d−d transitions in monomers is that they are Laporte forbidden. This is rigorous for **4**, as inversion site symmetry imposes C−Ni−C and P−Ni−P bond angles of 180°. In contrast, **2a** and **2b** show marked pyramidalization at the Ni atoms, with C−Ni−C and P−Ni−P angles of 175.9° and 176.5°, respectively, for **2a**, and 170.5° and 178.1°, respectively, for **2b**. This distortion may allow the single-centered d−d transitions to mix with higher-energy dipole-allowed transitions, thus promoting their intensity.

We note that our explanation for the lowest-energy bands of the dinuclear Ni(II) complexes does not invoke Ni−Ni interaction; instead, we attribute them to distortions from planarity at the Ni atoms imposed by the steric constraints of the bridging ligands. Indeed, we have found no evidence in the electronic spectra for significant Ni−Ni interaction.

Resonance Raman Studies. To further probe the metal−metal interactions of the dinuclear metal complexes, resonance Raman spectra of **1a** and **2a** have been recorded upon excitation into their lowest-energy dipole-allowed absorption bands. Figure 6 shows the resonance Raman spectrum of **1a** obtained in CH_2Cl_2 solution excited at 319.9 and 341.5 nm, respectively. The Raman intensity appears only in a single low-frequency mode plus overtones. The resonance-enhanced Raman band appears at $\Delta\nu = 93$ cm^{-1} and is assigned to the Pt−Pt stretch. This implies that the excited-state distortion is localized at the Pt−Pt bond, in agreement with the assignment of the metal-centered $5d_\sigma^* \rightarrow 6p_\sigma$ transition to the 337 nm absorption band for **1a** (see above) and previous work.[4,6] Moreover, this result contrasts sharply with resonance Raman studies of dinuclear Pt(II) complexes containing α-diimine ligands,[2d] which display resonance enhancement of α-diimine ligand modes upon excitation into the low-energy "metal−metal" transition band. This latter result

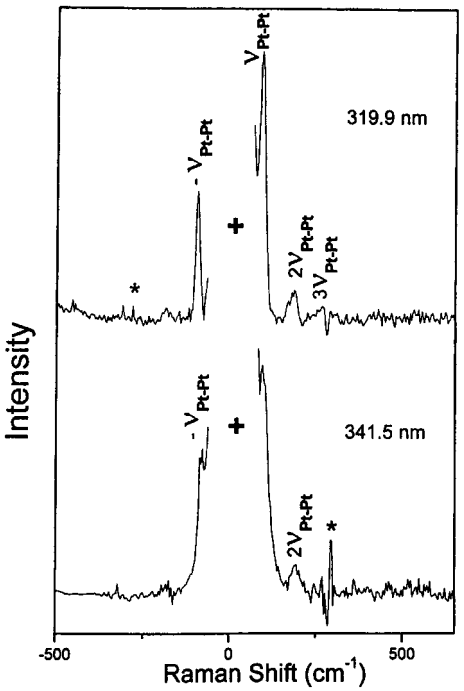

Figure 6. Resonance Raman spectra of **1a** in CH_2Cl_2 solution obtained with 319.9 and 341.5 nm excitation wavelengths. The spectra have been intensity corrected, and the Rayleigh line, glass bands (+ mark), and solvent bands (* mark) have been subtracted.

indicates substantial MLCT character for the transition, which is due to the low energy of empty diimine π^* orbitals.[2d,9g,i] When π^* ligand orbitals lie at substantially higher energies, as is true for the ligands in the present study according to electron-transmission spectroscopy,[33] the terminal orbital of the lowest-energy electronic transitions becomes virtually pure metal $(n + 1)$p in nature, and the characteristic pattern of almost exclusive resonance enhancement of $\nu(M_2)$ and overtones emerges. The validity of this argument is supported by transient-IR measurements on a dinuclear Rh(I) isocyanide complex,[34] which showed the ν(C≡N) value of the triplet excited state to be only 16 cm^{-1} lower than that of the ground state. Excited-state distortions involving ligands are accordingly predicted to be very small, hence resonance enhancement of the corresponding vibration modes should also be very small.

The smaller $\nu(Pt_2)$ (93 cm^{-1}) for **1a** compared with the value of 118 cm^{-1} in $[Pt_2(P_2O_5H_2)_4]^{4-}$ [6a] indicates weaker metal−metal interaction, consistent with the larger Pt···Pt distances in the former complex. The assigned $\nu(Pt_2)$ of 93 cm^{-1} can also be compared to the $\nu(Au_2)$ of 88 cm^{-1} for $[Au_2(dcpm)_2]^{2+}$ [35a] and $\nu(Ag_2)$ of 80 cm^{-1} for $[Ag_2(dcpm)_2]^{2+}$.[35b] Clearly the metal−metal bonding interaction in **1a** must be stronger than that in $[Au(I)]_2$ and $[Ag(I)]_2$. Using a previously described method of calculation,[6g] the

(32) Ballhausen, C. J.; Bjerrum, N.; Dingle, R.; Eriks, K.; Hare, C. R. *Inorg. Chem.* **1965**, *4*, 514−518.

(33) (a) Jordan, K. D.; Burrow, P. D. *Acc. Chem. Res.* **1978**, *11*, 341−348. (b) Burrow, P. D.; Ashe, A. J., III; Bellville, D. J.; Jordan, K. D. *J. Am. Chem. Soc.* **1982**, *104*, 425−429.

(34) Doorn, S. K.; Gordon, K. C.; Dyer, R. B.; Woodruff, W. H. *Inorg. Chem.* **1992**, *31*, 2284−2285.

(35) (a) Leung, K. H.; Phillips, D. L.; Tse, M.-C.; Che, C.-M.; Miskowski, V. M. *J. Am. Chem. Soc.* **1999**, *121*, 4799−4803. (b) Che, C.-M.; Tse, M.-C.; Chan, M. C. W.; Cheung, K.-K.; Phillips, D. L.; Leung, K. H. *J. Am. Chem. Soc.* **2000**, *122*, 2464−2468.

Table 4. Resonance Raman Bands of **1a** in CH_2Cl_2 Solution

		intensity[b]	
Raman bands	Raman shift (cm^{-1})[a]	319.9 nm	341.5 nm
$-2\nu_{Pt-Pt}$	−186		0.09
$-\nu_{Pt-Pt}$	−93	64	63
ν_{Pt-Pt}	93	100	100
absolute Raman cross section of ν_{Pt-Pt} ($Å^2$/molecule)			
expt		8.6×10^{-9}	9.25×10^{-9}
calcd[c]		3.58×10^{-9}	1.34×10^{-9}
calcd[d]		7.85×10^{-9}	1.25×10^{-9}
$2\nu_{Pt-Pt}$	186	22	18.4
$3\nu_{Pt-Pt}$	280		

[a] Estimated uncertainties are about 4 cm^{-1} for the wavenumbers. [b] Relative intensities are based on integrated areas of Raman bands. Estimated uncertainties are about 5% for intensities greater than 100, 10% for intensities between 50 and 100, and 20% for intensities below 50. [c] Calculated using the parameters of Table S2A (Supporting Information) with eq 1 and 2 in ref 6g and the exponential decay damping function for solvent dephasing. [d] Calculated using the parameters of Table S2B (Supporting Information) with eq 1 and 2 in ref 6g and the overdamped Brownian oscillator damping function for solvent dephasing.

excited-state Pt−Pt stretching vibration is estimated to be 145 cm^{-1}, which is in agreement with the electronic assignment of a transition to an excited state with increased metal−metal bonding. Using the parameters in Table 4 and a related calculation method,[6g] the Pt···Pt distances change by 0.11 Å for **1a** in the excited state relative to the ground-state value. The variation for the Pt−Pt bond length for **1a** is smaller than that of 0.225 Å for $[Pt_2(P_2O_5H_2)_4]^{4-}$.[6g]

The resonance Raman spectrum of **2a** in methanol with 416.0 nm excitation has also been recorded (see Supporting Information, Figure S6). The Raman intensity is very weak. The spectrum shows only two weak low-frequency peaks at −68 and 75 cm^{-1}, and no overtones appear. The −68 cm^{-1} feature is the quasi-anti-Stokes analogue of the 75 cm^{-1} band. These weak Raman peaks may be attributed to the Ni−Ni stretching vibration, although no overtone appears and the assignment is only tentative.

Theoretical Calculations. In this work, we have performed ab initio MP2 calculations on the molecules $[M_2(\mu\text{-}H_2PCH_2PH_2)_2(CN)_4]$ and *trans*-$[M(PMe_3)_2(CN)_2]$ (M = Pt, Ni). In the geometry optimization we have adopted different basis sets for the dinuclear and mononuclear model molecules, since their molecular sizes are different. The basis sets for the mononuclear compounds include d-polarization functions for second- and third-row atoms. For the dinuclear compounds, the basis sets are relatively small and no d-polarization functions were added for second- and third-row atoms. However, as described below, the optimized geometry parameters for both the mononuclear and dinuclear models are in good agreement with the corresponding bond distances and angles determined by X-ray crystal analysis. Furthermore, the d(P) orbital parentage in the *trans*-$[M(PMe_3)_2(CN)_2]$ frontier MO compositions is small. Previous work on the dinuclear $[Au_2(\mu\text{-}H_2PCH_2PH_2)_2]^{2+}$ complex[20] has indicated that the 3d(P) orbitals have little effect on the ground and excited states. Other theoretical calculations[31] on Pt−P or Pd−P systems have also revealed that the d-polarization functions for P atoms act as polarization functions and the d orbitals are not involved in metal-to-ligand charge transfer. The unimportant nature of 3d(P) orbitals in bonding[31d] is now understood to be very general; the low-energy σ^*(P−C) or (P−H) orbitals and not the 3d(P) orbitals are thought to act as π-acceptor orbitals according to current theories. We believe that the LANL2DZ basis sets with no d-polarization function added to P atoms are adequate, and they were used in the dinuclear calculations in order to reduce computational time and resources.

The optimized molecular structure parameters are summarized in Table 5. The calculated M···M distances of 3.1339 Å for Pt···Pt and 3.2447 Å for Ni···Ni are very similar to the experimental M···M distances of 3.189(1) and 3.209(8) Å found in complexes **1b** and **2b**, respectively. However, they deviate from the M···M distances of 3.0565(4) and 2.957(1) Å in **1a** and **2a**, respectively. The optimized $[M_2(\mu\text{-}H_2PCH_2PH_2)_2(CN)_4]$ structures are similar to the experimental data for $[M_2(dmpm)_2(CN)_4]$ complexes, and the shorter M···M distances in **1a** and **2a** compared to **1b** and **2b** are attributed to the steric effect of the dcpm ligand, as argued in a previous section. The other optimized structural parameters for the dinuclear and mononuclear models are consistent with the X-ray structural data. This indicates that the calculations give reasonable representations of the ground states.

The partial molecular orbital compositions for $[Pt_2(\mu\text{-}H_2PCH_2PH_2)_2(CN)_4]$ (see Table S5) and those for other model compounds are given in Supporting Information. The MO diagram of the Pt d-orbitals in $[Pt_2(\mu\text{-}H_2PCH_2PH_2)_2(CN)_4]$ is depicted in Figure 7. From Table S5 we can see that all the 5d(Pt) orbitals are involved in the filled MOs

Table 5. The Optimized Structural Data of the Model Complexes $[M_2(\mu\text{-}H_2PCH_2PH_2)_2(CN)_4]$ and *trans*-$[M(PMe_3)_2(CN)_2]$ (M = Pt, Ni)[a]

	Pt dimer [**1b**]	Ni dimer [**2b**]	Pt monomer [**3**]	Ni monomer [**4**]
		Bond Length (Å)		
M···M	3.1339 [3.189(1)]	3.2447 [3.209(8)]		
M−P	2.3606 [2.311(5)]	2.1798 [2.1984(4)]	2.3436 [2.336(1)]	2.2322 [2.2426(6)]
M−C	2.0224 [2.00(2)]	1.8413 [1.865(1)]	2.0066 [2.021(5)]	1.897 [1.857(3)]
C−N	1.2233 [1.185(4)]	1.2226 [1.145(2)]	1.1826 [1.105(7)]	1.2104 [1.148(4)]
P−C	1.8980 [1.88(2)]	1.9099 [1.832(1)]	1.8818 [1.849(5)]	1.8768 [1.852(2)]
		Bond Angle (deg)		
P−M−M	90.06 [89.25(1)]	91.76 [89.2]		
C−M−M	93.265 [91.975(8)]	93.178 [92.15]		
C−M−C	173.47 [175.6(7)]	173.64 [170.47(6)]	180.0 [180.0]	180.0 [180.0]
C−M−P	89.99 [87.7(7)]	92.44 [90.03(4)]	90.0 [90.0(1)]	90.0 [90.0(8)]
P−M−P	179.88 [178.3(1)]	176.49 [178.09(1)]	180.0 [180.0]	180.0 [180.0]

[a] The values within square brackets are the corresponding bond distances/bond angles of complexes **1b**, **2b**, **3**, and **4** determined by X-ray crystal analysis.

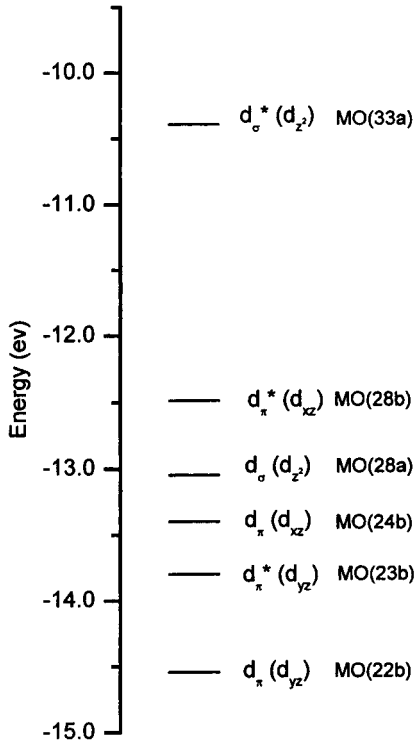

Figure 7. The calculated MO diagram of the partial Pt d-orbitals in $[Pt_2(\mu\text{-}H_2PCH_2PH_2)_2(CN)_4]$.

and contribute to the metal−metal and/or metal−ligand interactions. To check the metal−metal interaction, we pay attention to those MOs that have large metal parentage (>60%). The 22b and 24b MOs which have 81.4% d_{yz} and 87.0% d_{xz} character, respectively, are the π orbitals, and the 23b and 28b MOs with 73.1% d_{yz} and 78.1% d_{xz} character, respectively, are the π^* orbitals. These four MOs are responsible for the π type Pt−Pt interaction. However, they are fully occupied and there is no net π bonding. The δ bonding of Pt−Pt is not significant due to the small parentage of the d_{xy} and $d_{x^2-y^2}$ in the δ type MOs. The important feature would be the σ type metal−metal MOs. The rather large d_{z^2}−d_{z^2} overlap is found in 28a and 33a MOs, which have d_{z^2} compositions of 78.1% and 66.0%, respectively. There is more d_{z^2} contribution in the σ-bonding MO (28a) than in the σ^*-antibonding one (33a). The difference in d_{z^2} composition leads to σ-bonding interaction along the Pt−Pt axis. Furthermore, in the filled MOs there is small 6s6p parentage that would indirectly contribute to the metal−metal interaction.

Compared to $[Pt_2(\mu\text{-}H_2PCH_2PH_2)_2(CN)_4]$, the MO compositions of $[Ni_2(\mu\text{-}H_2PCH_2PH_2)_2(CN)_4]$ are not explicit for Ni−Ni bonding. However, comparing the MO compositions of the dinuclear and mononuclear model compounds, we can highlight one clear trend: the occupied MOs of dinuclear compounds are significantly less perturbed from those of the monomer for Ni than for Pt. The 3d(Ni) orbitals appear to be split by a few 1000 cm^{-1} (0.2−0.9 ev) in the dimer, whereas the 5d(Pt) orbitals undergo much larger splitting in the dimer (0.7−2.7 ev), particularly in the case of the predominately d_{z^2} parentage levels (2.66 eV, see Figure 7 and Tables S5 and S6 in the Supporting Information). This is consistent with Cotton's calculation[11] indicating negligible Ni−Ni interaction at a noticeably shorter intermetal distance (2.485 Å).

Acknowledgment. This work was supported by the University of Hong Kong and the Hong Kong Research Grants Council of the Hong Kong SAR (P.R. China) [HKU 7298/99P]. We thank Prof. Zhong-Yuan Zhou and Dr. Nian-Yong Zhu for some X-ray structural analyses and Dr. V. M. Miskowski for helpful discussions on spectroscopic assignments and comments on the manuscript.

Supporting Information Available: X-ray crystallographic file for all compounds in CIF format; selected bond distances and angles for compounds **3** and **4**; parameters for resonance Raman simulations for compound **1a**; calculated MO energies and orbital compositions for dimer and monomer model complexes; ORTEP diagrams for compounds **1a**, **1b**, **3**, and **4**; the resonance Raman spectrum of compound **2a** in methanol and related input and output gross orbital populations files for calculation. This material is available free of charge via the Internet at http://pubs.acs.org.

IC020077J